Hydrothermal Synthesis and Structural Characterization of V(III)-Containing Phases of the Vanadium Organodiphosphonate System. Crystal Structures of the V(III) Species $(H_3O)[V_3(O_3PCH_2CH_2PO_3)(HO_3PCH_2CH_2PO_3H)_3]$ and of the Mixed Valence V(III)/V(IV) Material $(H_3O)_2[(VO)V_2(OH)_2(O_3PCH_2CH_2PO_3)_2]\cdot H_2O$

Victoria Soghomonian,[†] Robert C. Haushalter,*[,‡] and Jon Zubieta*[,†]

Department of Chemistry, Syracuse University, Syracuse, New York 13244, and NEC Research Institute, 4 Independence Way, Princeton, New Jersey 08540

Received March 6, 1995. Revised Manuscript Received June 21, 1995[⊗]

The recent expansion of the chemistry of metal organophosphonate materials reflects their practical applications as sorbents, ion exchangers, catalysts, and hosts in intercalation compounds. Furthermore, the organophosphonate building blocks may be modified so as to allow the targeted design of solid-phase materials. The vanadium organophosphonate system provides a particularly rich structural chemistry which may be extended by exploiting linked diphosphonate groups with tethers of varying length or structure. Under reducing conditions, the introduction of octahedral V(III) sites into the mix of structural motifs further diversifies the structural chemistry of the system. In a typical preparation, the reaction of a mixture of VCl_4, $H_2O_3PCH_2CH_2PO_3H_2$, $H_2NC_2H_4NH_2$, and H_2O in the mole ratio 1:3.11:5.10:1890 at 200 °C for 87 h produced bright green truncated cubes of $(H_3O)[V_3(O_3PCH_2CH_2PO_3)(HO_3PCH_2CH_2PO_3H)_3]$ (**1**) and blue green plates of $(H_3O)_2[(VO)V_2(OH)_2(O_3PCH_2CH_2PO_3)_2]\cdot H_2O$ (**2**) in yields of 5% and 45%, respectively. The structure of **1** consists of layers of corner-sharing vanadium(III) octahedra $\{VO_6\}$ and phosphorus tetrahedra, pillared by the organic backbone of the ethylenediphosphonate groups. The polyhedral connectivity pattern results in the formation within the layers of cavities defined by the corner-sharing of six vanadium octahedra and six phosphorus tetrahedra and occupied by the hydronium cations. While the framework of **2** is similarly composed of V–P–O layers buttressed by the organic backbones of the ethylenediphosphonate groups, the layer structure is distinct from that of **1**. Compound **2** exhibits polyhedral connectivity resulting from the corner-sharing the V(III) octahedra, V(IV) square pyramids, and phosphorus tetrahedra which defines cavities constructed from four V(III), two V(IV), and four phosphorus polyhedral. Crystal data: **1**: $R\bar{3}c$, $a = 9.863(1)$, $c = 46.403(9)$, $V = 3090(2)$ Å^3, $Z = 6$, $D_{calc} = 2.346$ g/cm^3; structure refinement and solution based on 597 reflections (Mo Kα, $\lambda = 0.710\ 73$ Å) converged at $R = 0.0763$. **2**: $P\bar{1}$, $a = 7.150(1)$, b 7.809(2) Å, $c = 9.996(2)$ Å, $\alpha = 76.55(2)°$, $\beta = 70.17(2)°$, $\gamma = 88.91(2)°$, $V = 509.5(3)$ Å^3, $Z = 1$, $D_{calc} = 2.056$ g/cm^3; 1281 reflections, $R = 0.0740$.

The general interest in the chemistry of metal organophosphonates stems in part from the unusual structural diversity associated with monomolecular coordination complexes[1] and molecular clusters,[2,3] one-dimensional complexes,[4] layered compounds,[5,6] and even three-dimensional phases.[7] Furthermore, metal organophosphonate materials possess a variety of practical applications as catalysts, hosts in intercalation compounds, sorbents, ion exchangers, and solvolytically stable films with optical, nonlinear optical, and electronic properties.[8–23]

[†] Syracuse University.
[‡] NEC Research Institute.
[⊗] Abstract published in *Advance ACS Abstracts,* August 1, 1995.

(1) Clark, E. T.; Rudolf, P. R.; Martell, A. E.; Clearfield, A. *Inorg. Chem. Acta* **1989**, *164*, 59 and references therein.
(2) Zubieta, J. *Comments Inorg. Chem.* **1994**, *16*, 153 and references therein.
(3) Chen, Q.; Salta, J.; Zubieta, J. *Inorg. Chem.* **1993**, *32*, 4485 and references therein.
(4) Bujoli, B.; Palvadeau, P.; Rouxel, J. *Chem. Mater.* **1990**, *2*, 582 and references therein.
(5) Bhardwaj, C.; Hu, H.; Clearfield, A. *Inorg. Chem.* **1993**, *32*, 4294 and references therein.
(6) Zhang, Y.; Clearfield, A. *Inorg. Chem.* **1992**, *31*, 2821.
(7) Bideau, J. L.; Payen, C.; Palvadeau, P.; Bujoli, B. *Inorg. Chem.* **1994**, *33*, 4885.
(8) Lowe, M. P.; Lockhart, J. C.; Clegg, W.; Fraser, K. A. *Angew. Chem., Int. Ed. Engl.* **1994**, *33*, 451.
(9) Alberti, G.; Constantino, U.; Marmottini, F.; Vivani, R.; Zappelli, P. *Angew. Chem.* **1993**, *105*, 1396; *Angew. Chem., Int. Ed. Engl.* **1993**, *32*, 1357 and references therein.
(10) Alberti, G.; Constantino, U. In *Inclusion Compounds 5*; Atwood, J. L., Davis, J. E. D., MacNicol, D. D., Eds.; Oxford University Press: Oxford, 1991; Chapter 5.
(11) Burwell, D. A.; Thompson, M. E. In *Supramoleclar Architecture; ACS Symp. Ser.* **1992**, *499*, 166.
(12) Clearfield, A.; Ortiz-Avila, C. Y. In *Supramolecular Architecture; ACS Symp. Ser.* **1992**, *499*, 178.
(13) Clearfield, A. *Inorganic Ion Exchange Materials*; CRC Press: Boca Raton, FL, 1982; p 1.
(14) Clearfield, A. In *Design of New Materials*. Cocke, D. L.; Clearfield, A., Eds.; Plenum: New York, 1986.
(15) Rosenthal, G. L.; Caruso, J. *Inorg. Chem.* **1992**, *31*, 144.

0897-4756/95/2807-1648$09.00/0

The vanadium organophosphonate system has proved particularly fruitful, yielding a variety of complex molecular clusters of nuclearities 2–18[2,3,24–29] and of solid phases with 1-dimensional, 2-dimensional, and 3-dimensional framework.[30–35] We have recently demonstrated that the chemistry of the vanadyl organophosphonate system can be dramatically expanded by the introduction of cationic templating reagents as structure-directing substrates and by the manipulation of tether length and structure of organodiphosphonate groups, $R'(PO_3)_2^{4-}$.[30] However, while the structural diversity of the oxovanadium(IV,V) organophosphonate system is apparent from these numerous reports, V(III)-containing organophosphonate phases have remained elusive. Herein, we report the first structurally characterized V(III) organophosphonate solids, $(H_3O)[V_3(O_3PCH_2CH_2PO_3)(HO_3PCH_2CH_2PO_3H)_3]$ (**1**) and the mixed valence V(III,IV) species $(H_3O)_2[(VO)V_2(OH)_2(O_3PCH_2CH_2PO_3)]\cdot H_2O$ (**2**). While both structures may be described grossly as 2-D V–P–O networks "pillared" by the organic backbones of the diphosphonate units, the structural details within the V–P–O layers are quite distinct.

Experimental Section

Hydrothermal reactions were carried out in Parr acid digestion bombs with 23 mL poly(tetrafluoroethylene) liners or in borosilicate tubes with 15 mm outer diameter, 11 mm inner diameter, and length of 254 mm. Ethylenediamine, ethylenediphosphonic acid, and VCl_4 were purchased from Aldrich. The VCl_4 was carefully hydrolyzed by addition over 0.5 h to water cooled to 4 °C in an ice bath to give a turquoise solution of "VO^{2+}" which was used as the vanadium(IV) source. The concentration of the solution was 1.47 M. Infrared spectra were obtained on a Perkin-Elmer 1600 Series FTIR spectrometer.

Synthesis of Compounds. *Synthesis of $(H_3O)[V_3(O_3PCH_2CH_2PO_3)(HO_3PCH_2CH_2PO_3H)_3]$ (1) and $(H_3O)_2[(VO)V_2(OH)_2(O_3PCH_2CH_2PO_3)_2]\cdot 2H_2O$ (2).* A mixture of VCl_4, ethylenediphosphonic acid, ethylenediamine, and H_2O (10 mL, 44% fill volume) in the mole ratio 1:3.11:5.10:1890 was heated at 200 °C for 87 h in a Parr bomb. Blue green plates of **2**, contaminated by bright green truncated cubes of **1**, were collected and mechanically separated. The yield of **2** was 45%, based on vanadium, with **1** present in ca. 5% yield.

Attempts to isolate either **1** or **2** as monophasic materials proved unsuccessful. The optimal conditions for the synthesis of **2** are those detailed above. Neither variations in stoichiometries nor use of other organoamines improved yield or purity. The yield of **1** was not appreciably improved by addition of reduced vanadium starting materials, either as vanadium metal (−325 mesh) or as VCl_3 in rigorously degassed glass ampules. Anal. Calcd for $C_8H_{25}O_{25}P_8V_3$ (**1**): C, 10.4; H, 2.71. Found: C, 10.2; H, 3.00. IR (KBr pellet, cm^{-1}) 3438 (s, br), 3283 (m), 2929 (w), 1634 (w), 1424 (m), 1252 (s), 1191 (s), 1147 (s), 985 (s), 926 (w), 760 (m), 715 (w), 571 (m), 555 (m), 521 (m), 477 (s). Anal. Calcd for $C_4H_{18}O_{18}P_4V_3$ (**2**): C, 7.61; H, 2.85. Found: C, 7.82; H, 2.51. IR (KBr pellet, cm^{-1}) 3452 (m, br), 2927 (w), 1200 (m), 1088 (s), 1043 (s), 993 (s), 875 (s), 764 (w), 523 (m, br).

X-ray Crystallographic Studies. The experimental X-ray data for the structures of **1** and **2** are summarized in Table 1; atomic coordinates are listed in Table 2 and 3, and selected bond lengths and angles are presented in Tables 4 and 5.

Data are collected on a Rigaku AFC5S four-circle diffractometer. In the case of **2**, crystal stability was considerably improved by cooling to −40 °C. In neither case was significant crystal decomposition observed during the course of the data collection.

Table 1. Crystallographic Data for the Structural Studies of $(H_3O)[V_3(O_3PCH_2CH_2PO_3)(HO_3PCH_2CH_2PO_3H)_3]$ (1) and $(H_3O)_2[(VO)V_2(OH)_2(O_3PCH_2CH_2PO_3)_2]\cdot H_2O$ (2)

	1	2
chemical formula	$C_8H_{25}O_{25}P_8V_3$	$C_4H_{18}O_{18}P_4V_3$
a, Å[a]	9.863(1)	7.150(1)
b, Å	9.863(1)	7.809(2)
c, Å	46.403(9)	9.996(2)
α, deg	90.0	76.55(2)
β, deg	90.0	70.17(2)
γ, deg	120.0	88.91(2)
V, Å^3	3909(2)	509.5(3)
Z	6	1
formula weight	921.9	630.9
space group	$R\bar{3}c$	$P\bar{1}$
T, °C	23	−40
λ, Å[b]	0.71073	0.71073
D_{calc}, g cm^{-3}	2.346	2.056
μ, cm^{-1}	16.64	17.51
R^c	0.0763	0.0740
$R_w{}^d$	0.0831	0.0880

[a] Lattice parameters based on the angle settings of 25 reflections with $20° \le 2\theta \le 45°$. [b] Absorption corrections based on φ scans for 5 reflections with χ angles near 90° or 270°. [c] $\sum||F_o| - |F_c||/\sum|F_o|$. [d] $[\sum w(|F_o| - |F_c|)^2/\sum w|F_o|^2]^{1/2}$.

Table 2. Atomic Coordinates ($\times 10^4$) and Equivalent Isotropic Displacement Coefficients (Å$^2 \times 10^3$) for $(H_3O)[V_3(O_3PCH_2CH_2PO_3)(HO_3PCH_2CH_2PO_3H)_3]$ (1)

	x	y	z	U(eq)[a]
V(1)	0	−5792(4)	2500	12(1)
P(1)	6667	3333	8813(1)	16(2)
P(2)	5834(5)	307(5)	9553(1)	11(2)
O(1)	1584(14)	1385(13)	580(2)	26(6)
O(2)	4428(14)	4336(13)	597(2)	22(5)
O(3)	5703(14)	7302(13)	575(2)	23(6)
O(4)	7150(14)	5868(14)	441(3)	25(6)
O(5)	−496(35)	0	2500	15(11)
C(2)	4947(19)	5689(18)	72(3)	18(3)
C(1)	16(58)	−692(38)	125(7)	44(12)

[a] Equivalent isotropic U defined as one-third of the trace of the orthogonalized U_{ij} tensor.

(16) Burwell, D. A.; Valentine, K. G.; Timmermans, J. H.; Thompson, M. E. *J. Am. Chem. Soc.* **1992**, *114*, 414.
(17) Gao, G.; Mallouk, T. E. *Inorg. Chem.* **1991**, *30*, 1434.
(18) Wang, R.-C.; Zhang, Y.; Hu, H.; Frausto, R. R.; Clearfield, A. *Chem. Mater.* **1992**, *4*, 864.
(19) Lee, H.; Keply, T. J.; Hong, H.-G.; Akhter, S.; Mallouk, T. G. *J. Phys. Chem.* **1988**, *92*, 2597.
(20) Yang, H. C.; Aoki, K.; Hong, H.-G.; Sackett, D.; Arendt, M. F.; Yan, S.-L.; Bell, C. M.; Mallouk, T. E. *J. Am. Chem. Soc.* **1993**, *115*, 11855.
(21) Katz, H. E.; Wilson, W. L.; Scheller, G. *J. Am. Chem. Soc.* **1994**, *116*, 6636.
(22) Ungashe, S. B.; Wilson, W. L.; Katz, H. E.; Scheller, G. R.; Putrinski, T. M. *J. Am. Chem. Soc.* **1992**, *114*, 8717.
(23) Byrd, H.; Pike, J. K.; Talham, D. R. *J. Am. Chem. Soc.* **1994**, *116*, 7903.
(24) Chen, Q.; Zubieta, J. *J. Chem. Soc., Chem. Commun.* **1994**, 2663.
(25) Salta, J.; Chen, Q.; Chang, Y.-D.; Zubieta, J. *Angew. Chem., Int. Ed. Engl.* **1994**, *33*, 757.
(26) Chen, Q.; Zubieta, J. *Angew. Chem., Int. Ed. Engl.* **1993**, *32*, 261.
(27) Khan, M. I.; Chang, Y.-D.; Chen, Q.; Höpe, H.; Parkin, S.; Goshorn, D. P.; Zubieta, J. *Angew. Chem., Int. Ed. Engl.* **1992**, *31*, 1197.
(28) Chang, Y.-D.; Salta, J.; Zubieta, J. *Angew. Chem., Int. Ed. Engl.* **1994**, *33*, 325.
(29) Khan, M. I.; Zubieta, J. *Angew. Chem., Int. Ed. Engl.* **1994**, *33*, 760.
(30) Soghomonian, V.; Chen, Q.; Haushalter, R. C.; Zubieta, J. *Angew. Chem., Int. Ed. Engl.* **1995**, *34*, 223.
(31) Huan, G.; Jacobson, A. J.; Johnson, J. W.; Corcoran, E. W., Jr. *Chem. Mater.* **1990**, *2*, 91.
(32) Khan, M. I.; Lee, Y.-S.; O'Connor, C. J.; Haushalter, R. C.; Zubieta, J. *J. Am. Chem. Soc.* **1994**, *116*, 4525.
(33) Khan, M. I.; Lee, Y.-S.; O'Connor, C. J.; Haushalter, R. C.; Zubieta, J. *Chem. Mater.* **1994**, *6*, 721.
(34) Khan, M. I.; Lee, Y.-S.; O'Connor, C. J.; Haushalter, R. C.; Zubieta, J. *Inorg. Chem.* **1994**, *33*, 3855.
(35) Huan, G.; Johnson, J. W.; Jacobson, A. J.; Merola, J. S. *J. Solid State Chem.* **1990**, *89*, 220.

Table 3. Atomic Coordinates ($\times 10^4$) and Equivalent Isotropic Displacement Coefficients ($Å^2 \times 10^3$) for $(H_3O)_2[(VO)V_2(OH)_2(O_3PCH_2CH_2PO_3)_2]\cdot H_2O$ (2)

	x	y	z	U(eq)[a]
V(1)	0	0	0	28(1)
V(2)	5000	0	0	38(1)
V(3)	4436(5)	−32(6)	5060(5)	14(1)
P(1)	3310(4)	−2439(3)	−1561(3)	18(1)
P(2)	3708(4)	2380(3)	7319(3)	19(1)
O(1)	1173(11)	−2007(9)	9147(8)	21(3)
O(2)	5326(11)	2063(10)	10776(9)	30(3)
O(3)	4132(18)	−1502(10)	6823(9)	49(5)
O(4)	1553(10)	1697(9)	8172(8)	20(3)
O(5)	5089(11)	1647(10)	8146(9)	26(3)
O(6)	4387(14)	2071(10)	5795(8)	36(3)
O(7)	2302(26)	−113(23)	5050(17)	53(8)
O(8)	2159(10)	86(9)	10726(8)	18(3)
O(9)	1257(25)	2914(22)	2425(18)	33(4)
O(10)	1275(30)	6102(26)	2699(23)	55(6)
O(11)	−429(80)	3685(68)	5453(62)	66(24)
C(1)	6732(19)	4800(13)	11386(11)	25(4)
C(2)	3804(20)	4744(14)	7074(12)	30(5)

[a] Equivalent isotropic U defined as one-third of the trace of the orthogonalized U_{ij} tensor.

Table 4. Bond Lengths (Å) and Angles (deg) for 1

V(1)−O(1A)	2.039 (11)	V(1)−O(1B)	2.039 (11)
V(1)−O(2A)	2.008 (15)	V(1)−O(2B)	2.008 (12)
V(1)−O(3A)	1.965 (11)	V(1)−O(3B)	1.965 (7)
P(1)−O(1A)	1.545 (10)	P(1)−O(1B)	1.546 (15)
P(1)−O(1A)	1.545 (9)	P(1)−C(1)	1.784 (34)
P(2)−O(2)	1.498 (13)	P(2)−O(3)	1.494 (10)
P(2)−O(4)	1.585 (16)	P(2)−C(2)	1.814 (16)
C(2)−C(2A)	1.565 (40)	C(1)−C(1a)	1.453 (41)
O(1A)−V(1)−O(1B)	174.5(8)	O(1A)−V(1)−O(2B)	89.9(5)
O(1B)−V(1)−O(2B)	86.1(5)	O(1A)−V(1)−O(2C)	86.1(5)
O(1B)−V(1)−O(2C)	89.9(5)	O(2B)−V(1)−O(2C)	87.7(7)
O(1A)−V(1)−O(3A)	91.3(5)	O(1B)−V(1)−O(3A)	92.4(5)
O(2B)−V(1)−O(3A)	88.5(5)	O(2C)−V(1)−O(3A)	175.4(5)
O(1A)−V(1)−O(3C)	92.4(5)	O(1B)−V(1)−O(3C)	91.3(5)
O(2B)−V(1)−O(3C)	175.4(5)	O(2C)−V(1)−O(3C)	88.5(5)
O(3A)−V(1)−O(3C)	95.4(8)	O(1C)−P(1)−O(1D)	111.4(5)
O(1C)−P(1)−O(1E)	111.4(6)	O(1D)−P(1)−O(1E)	111.4(4)
O(1C)−P(1)−C(1F)	114.7(14)	O(1D)−P(1)−C(1G)	114.6(18)
O(2A)−P(2)−O(3B)	116.5(7)	O(2A)−P(2)−O(4A)	104.7(7)
O(3B)−P(2)−O(4A)	111.1(8)	O(2A)−P(2)−C(2B)	109.0(8)
O(3B)−P(2)−C(2B)	109.8(6)	O(4A)−P(2)−C(2B)	105.1(8)
V(1B)−O(1)−P(1A)	140.4(9)	V(1B)−O(2)−P(2A)	141.7(10)
V(1A)−O(3)−P(2A)	154.0(10)	P(2A)−C(2)−C(2A)	108.8(17)
P(1A)−C(1)−C(1A)	107.4(35)		

In both cases, data were corrected for Lorentz, polarization, and absorption effects in the usual fashion. Both structures were solved by Patterson techniques and refined by full-matrix least squares using SHELXTL. In both cases, refinement proceeded routinely, and no anomalies in temperature factors or excursions of electron density in the final Fourier maps were observed.

Minor disorder effects were encountered in the structural analyses of both **1** and **2**. For **1**, the ethylene bridge associated with the P1 sites (C1 and C1a) is disordered about the crystallographic $\bar{3}$ axis. The disorder was adequately modeled by assigning 0.33 occupancy to this site. In the case of **2**, the oxovanadium(IV) unit, V1−O1, disorders about the inversion center. Again, adjusting the site population to 0.5 proved satisfactory, and no unusual excursions of electron density were observed along the V−O axis.

Results and Discussion

Synthesis and Infrared Characterization. The solid-state chemistry of both the oxovanadium phosphate and oxovanadium organophosphonate systems[30-37] has been significantly expanded by the application of the techniques of hydrothermal synthesis,[38] which not only provide a low-temperature pathway to metastable structures utilizing simple inorganic and organic precursors of desired geometry but also allow the introduction of templating agents for the organization of networks of oxovanadium polyhedra and phosphorus tetrahedra. While the phases described previously featured exclusively oxovanadium(IV) and/or -(V) sites as constituents of the V−P−O network, the existence of numerous V(III)-containing phases of the analogous $V-O-PO_4^{3-}$ system[39,40] suggested that V(III) sites could be incorporated into the vanadium organophosphonate system under appropriate conditions. Since the identities of the products isolated by hydrothermal syntheses are critically dependent on reaction conditions and since the parameter space associated with the hydrothermal technique is vast, factors such as temperature, stoichiometries, pH, fill volume, surface nucleation, nature of the oxometal source, and templating reagents contribute to the product formation. Consequently, reducing con-

Table 5. Bond Lengths (Å) and Angles (deg) for 2

V(1)−O(1)	1.993 (8)	V(1)−O(1A)	1.993 (8)
V(1)−O(4)	1.970 (6)	V(1)−O(4A)	1.970 (6)
V(1)−O(8)	1.924 (9)	V(1)−O(8A)	1.924 (9)
V(2)−O(2)	1.993 (9)	V(2)−O(2A)	1.993 (9)
V(2)−O(5)	1.977 (8)	V(2)−O(5A)	1.977 (8)
V(2)−O(8A)	1.917(7)	V(2)−O(8B)	1.917 (7)
V(3)−O(3)	1.810 (9)	V(3)−O(6)	1.944 (10)
V(3)−O(7)	1.532 (20)	V(3)−O(3A)	1.928 (8)
V(3)−O(6A)	2.017 (9)	P(1)−O(1)	1.519 (8)
P(1)−O(2)	1.514 (11)	P(1)−O(3)	1.521 (8)
P(1)−C(1)	1.811 (11)	P(2)−O(4)	1.521 (7)
P(2)−O(5)	1.516 (10)	P(2)−O(6)	1.510 (8)
P(2)−C(2)	1.804 (11)	C(1)−C(2)	1.579 (17)
O(1A)−V(1)−O(1B)	180.0(1)	O(1A)−V(1)−O(4A)	90.5(3)
O(1B)−V(1)−O(4A)	89.5(3)	O(1A)−V(1)−O(4B)	89.5(3)
O(1B)−V(1)−O(4B)	90.5(3)	O(4A)−V(1)−O(4B)	180.0(1)
O(1A)−V(1)−O(8A)	89.9(3)	O(1B)−V(1)−O(8A)	90.1(3)
O(4A)−V(1)−O(8A)	89.6(3)	O(4B)−V(1)−O(8A)	90.4(3)
O(1A)−V(1)−O(8B)	90.1(3)	O(1B)−V(1)−O(8B)	89.9(3)
O(4A)−V(1)−O(8B)	90.4(3)	O(4B)−V(1)−O(8B)	89.6(3)
O(8A)−V(1)−O(8B)	180.0(1)	O(2A)−V(2)−O(2B)	180.0(1)
O(2A)−V(2)−O(5A)	89.1(4)	O(2B)−V(2)−O(5A)	90.9(4)
O(2A)−V(2)−O(5B)	90.9(4)	O(2B)−V(2)−O(5B)	89.1(4)
O(5A)−V(2)−O(5B)	180.0(1)	O(2A)−V(2)−O(8A)	90.9(3)
O(2B)−V(2)−O(8A)	89.1(3)	O(5A)−V(2)−O(8A)	89.4(3)
O(5B)−V(2)−O(8A)	90.6(3)	O(2A)−V(2)−O(8C)	89.1(3)
O(2B)−V(2)−O(8C)	90.9(3)	O(5A)−V(2)−O(8C)	90.6(3)
O(5B)−V(2)−O(8C)	89.4(3)	O(8A)−V(2)−O(8C)	180.0(1)
O(3)−V(3)−O(6)	93.1(4)	O(3)−V(3)−O(7)	100.7(7)
O(6)−V(3)−O(7)	99.7(8)	O(3)−V(3)−O(3B)	156.4(2)
O(6)−V(3)−O(3B)	84.7(4)	O(7)−V(3)−O(3B)	102.9(7)
O(3)−V(3)−O(6A)	85.8(4)	O(6)−V(3)−O(6A)	157.5(2)
O(7)−V(3)−O(6A)	102.6(8)	O(1A)−P(1)−O(2B)	113.0(5)
O(1A)−P(1)−O(3A)	111.3(6)	O(2B)−P(1)−O(3A)	110.8(6)
O(1A)−P(1)−C(1A)	106.6(5)	O(2B)−P(1)−C(1A)	105.7(6)
O(3A)−P(1)−C(1A)	109.0(5)	O(4)−P(2)−O(5)	112.1(4)
O(4)−P(2)−O(6)	111.4(5)	O(5)−P(2)−O(6)	112.3(5)
O(4)−P(2)−C(2)	107.2(5)	O(5)−P(2)−C(2)	107.7(6)
O(6)−P(2)−C(2)	105.7(5)	V(1A)−O(1)−P(1A)	132.5(5)
V(2A)−O(2)−P(1B)	131.7(5)	V(3)−O(3)−P(1A)	162.6(8)
V(3A)−O(3)−P(1A)	165.6(8)	P(2)−O(4)−V(1A)	139.0(5)
P(2)−O(5)−V(2A)	139.8(4)	V(3)−O(6)−P(2)	133.0(4)
P(2)−O(6)−V(3A)	134.0(5)	V(1A)−O(8)−V(2A)	137.1(4)
P(1B)−C(1)−C(2A)	111.5(6)	P(2)−C(2)−C(1B)	109.5(6)

(36) Soghomonian, V.; Chen, Q.; Haushalter, R. C.; Zubieta, J.; O'Connor, C. J. *Science* **1993**, *259*, 1596.
(37) Soghomonian, V.; Haushalter, R. C.; Chen, Q.; Zubieta, J. *Inorg. Chem.* **1994**, *33*, 1700 and references therein.
(38) Rouxel, J. *Chem. Scripta* **1988**, *28*, 33 and references therein.
(39) Haushalter, R. C.; Wang, Z.; Thompson, M. G.; Zubieta, J. *Inorg. Chem.* **1993**, *32*, 3700.
(40) Lii, K. H.; Wen, N. S.; Su, C. C.; Chen, B. R. *Inorg. Chem.* **1992**, *31*, 439 and references therein.

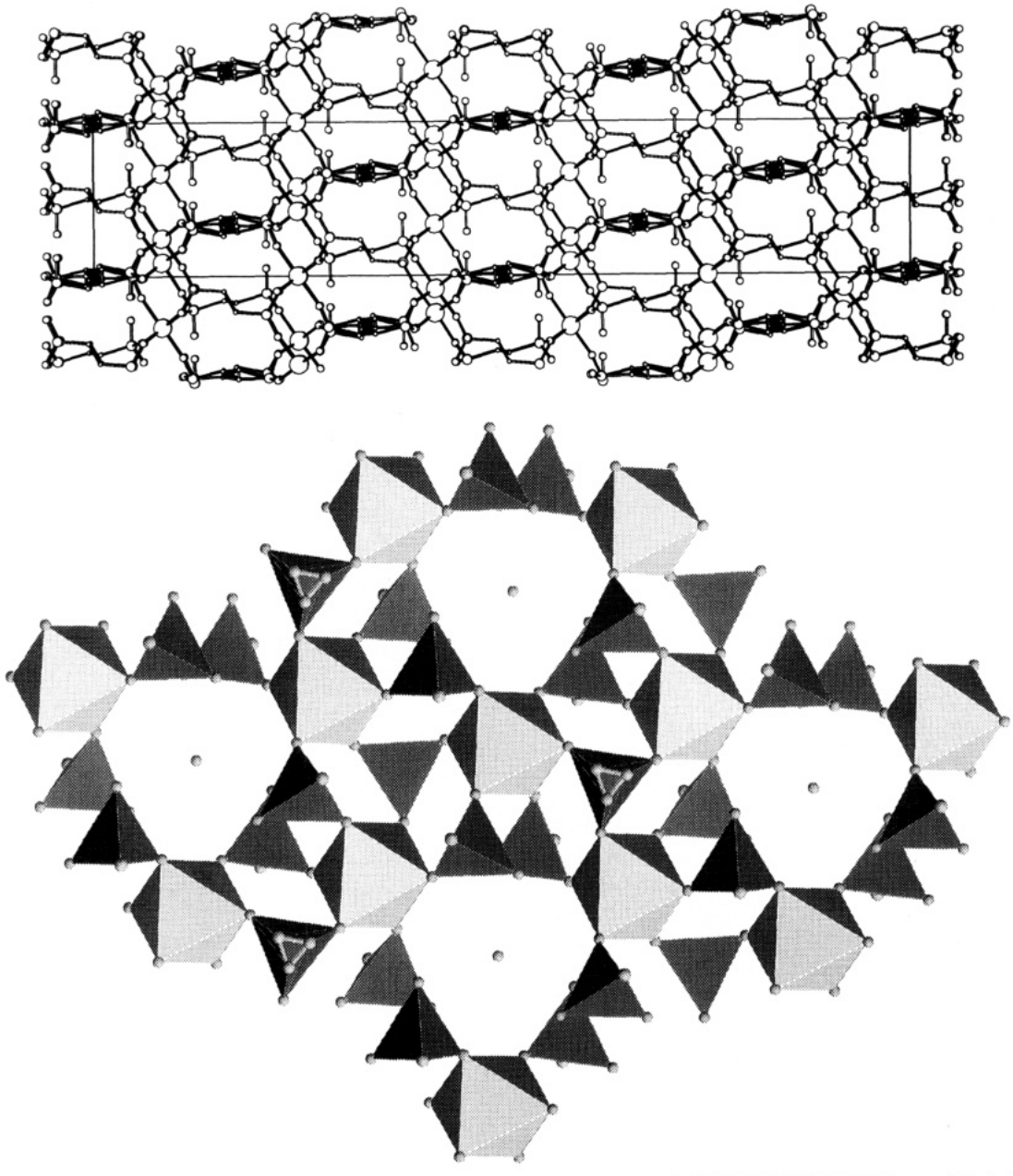

Figure 1. (a, top) View of the unit-cell contents of $(H_3O)[V_3(O_3PCH_2CH_2PO_3)(HO_3PCH_2)CH_2PO_3H)_3]$ (**1**) parallel to (0001). The atoms are represented by circles of diminishing size: vanadium, phosphorus, oxygen, carbon. The disorder of the C1 site about the $\bar{3}$ axis is apparent. (b, bottom) Polyhedral view of the V−P−O layer of **1**, showing the location of the H_3O^+ cation.

ditions may be used to favor the isolation of lower valent vanadium organophosphonate phases, an observation which has led the to isolation of two V(III)-containing phases, $(H_3O)[V_3(O_3PCH_2CH_2PO_3)(HO_3PCH_2CH_2PO_3H)_3]$ (**1**) and $(H_3O)_2[(VO)V_2(OH)_2(O_3PCH_2CH_2PO_3)_2]\cdot H_2O$ (**2**).

The compounds are isolated in the reaction of VCl_4, ethylenediphosphonate, ethylenediamine, and H_2O at 200 °C. We have previously noted[32,41] that organoamines function as reducing agents in hydrothermal reactions involving V(IV) or V(V) precursors, particularly in the higher temperature domain (180−220 °C). While the identity of the oxidized organic product has not been determined, it has been established that neither **1** or **2** form under similar reaction conditions to those described in the absence of an organoamine reactant. Furthermore, while microcrystalline mixtures of blue-green products were isolated using organoamines other than ethylenediamine, separable crystalline forms were produced only in the presence of ethylenediamine. Efforts to isolate **1** as a monophasic material proved unsuccessful. Mixtures of VCl_4 and vanadium metal or the use of degassed VCl_3 solutions produced only amorphous tan materials. Consequently, **1** was isolated only as a minor component (ca. 10%) from the preparation of **2**, which may be isolated in 50% yield under optimal conditions. Since the colors and crystal shapes of **1** and **2** are quite distinct, the materials were readily separated mechanically.

The infrared spectrum of **1** exhibited a strong band at 3438 cm^{-1} associated with ν(O−H) of the hydronium cation and a set of four intense bands in the 980−1200 cm^{-1} region attributed to ν(P−O) of the diphosphonate groups. The absence of features of significantly intensity in the 800−950 cm^{-1} region suggested the absence

(41) Khan, M. I.; Haushalter, R. C.; O'Connor, C. J.; Tao, C.; Zubieta, J. *Chem. Mater.* **1995**, *7*, 593.

of vanadium-terminal oxo units which are ubiquitous in the V(IV) and V(V) phases. The spectrum of **2** likewise possesses infrared bands at 3452 cm^{-1} and in the 990−1200 cm^{-1} region attributed to hydronium ν(O−H) and diphosphonate ν(P−O) stretching frequencies. In addition, a strong band at 875 cm^{-1} is attributed to ν(V=O).

Structural Descriptions. Although the coordination chemistry of vanadium is dominted by the oxophilicity of the metal in the +4 and +5 oxidation states,[42] the +3 oxidation state is readily accessible in aqueous solution. The coordination geometries at vanadium centers are highly variable: V(IV) and V(V) may adopt tetrahedral, square-pyramidal, trigonal-bipyramidal, and octahedral geometries, while V(III) species characteristically assume octahedral geometries. Although multiply bonded terminal oxo groups {V=O} with short V−O distances (ca. 1.60 Å) are ubiquitous to the V(IV)- and V(V)-containing phases, V(III) species do not exhibit such interactions and the distances in {VO_6} octahedra fall in a narrow range of ca. 1.90−2.10 Å. These general geometric features are evident in the structures of both **1** and **2**.

The structure of the anionic framework of **1** may be described in terms of V−P−O layers of corner-sharing {VO_6} octahedra and phosphorus tetrahedra pillared by the organic backbone {$-CH_2CH_2-$} of the organodiphosphonate groups, with an interlamellar separation of 7.73 Å as shown in Figure 1a. The polyhedral connectivity within the layers, shown in Figure 1b, reflects the presence of two distinct organodiphosphonate types. As illustrated in Figure 2a, the P1 sites coordinate to each of three adjacent vanadium sites through each of the three oxygen donors, while the P2 sites bridge two adjacent vanadium sites within a layer and exhibit a pendant protonated {P−OH} unit, as indicated by the P−O distance of 1.60(2) Å, compared to an average P−O distance of 1.51(2) Å for the phosphate oxygens involved in bonding to the vanadium centers. Consequently, each vanadium site coordinates to six oxygen donors, each from a different organophosphonate groups. Four oxygen donors to each vanadium are contributed by P2 sites and two by P1 sites, to produce a layer motif in which each vanadium site bridges through two symmetrically bridging {V−O−P−O−V} interactions to each of four adjacent vanadium centers. The vanadium-oxygen distances fall in the range 1.97−2.04 Å, and the valence sum calculations[42] confirm that the metal is present in the +3 oxidation state.

This pattern of octahedral−tetrahedral connectivity within each V−P−O plane results in the formation of cavities bound by six phosphate tetrahedra and six vanadium octahedra, as shown in Figure 2b. The six pendant −OH groups of the organodiphosphonate ligands provide the boundary of a hydrophilic cavity which is occupied by the hydronium cation. The close contacts between the hydronium O5 and the oxygen atoms of the cavity perimeter indicate that hydrogen-bonding interactions are significant (Table 6).

It is noteworthy that the requirement that the organodiphosphonate groups bridge adjacent V−P−O layers constrains the phosphonate tetrahedra to occupy positions above and below the plane of the vanadium octahedra. Consequently, each V−P−O layer, as presented in Figure 2c, is three polyhedra thick, with the vanadium layer of octahedra sandwiched between layers of phosphonate tetrahedra.

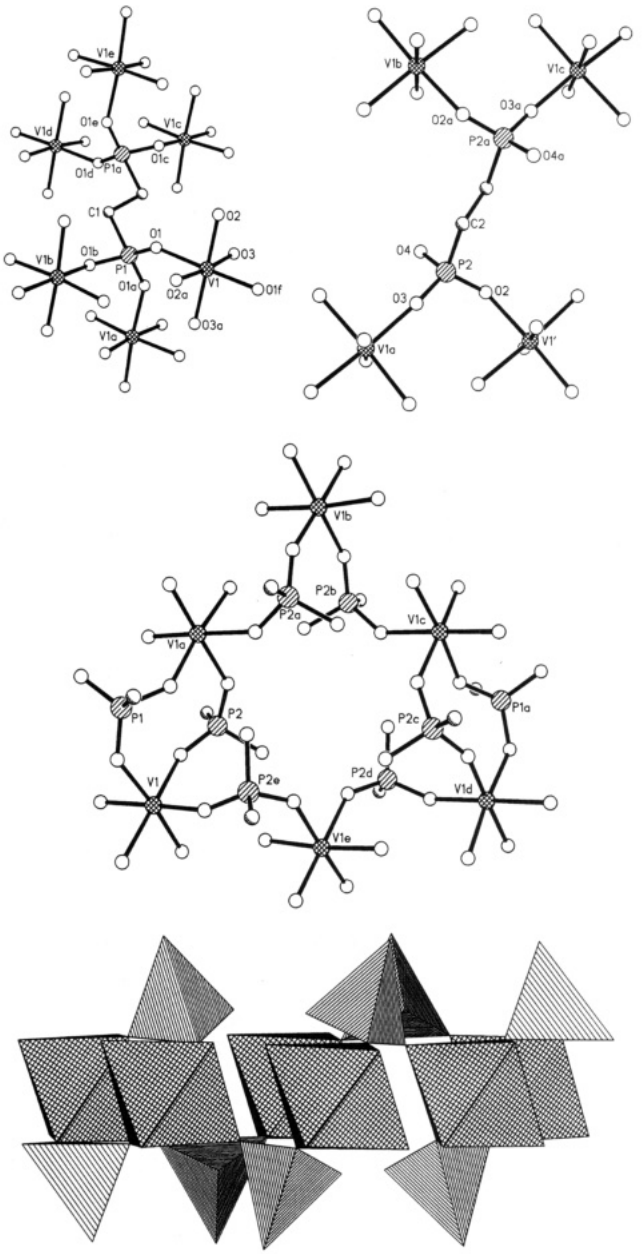

Figure 2. (a, top) Schematic representations of the two organodiphosphonate groups of **1**, showing the atom-labeling scheme. (b, middle) View of a cavity generated in the V−P−O layer via corner-sharing the six vanadium octahedra and six P2 tetrahedra and showing the location of the pendant −OH groups. (c, bottom) Polyhedral view of the ring of **2**(b), highlighting the three-polyhedra thickness of the layer.

Table 6. Listing of Contacts for the Hydronium Oxygen Atoms of 1 and 2

(a) $(H_3O)[V_3(O_3PCH_2CH_2PO_3)(HO_3PCH_2CH_2PO_3)_3]$ (**1**)	
O5···O4	2.57(1)
O5···O2	2.73(1)
(b) $(H_3O)_2[(VO)V_2(OH)_2(O_3PCH_2CH_2PO_3)_2]\cdot H_2O$ (**2**)	
O9···O10	2.57(1)
O10···O11	2.83(1)
O10···O4	2.84(1)
O10···O5	2.92(1)

(42) Brown, I. D. In *Structure and Bonding in Crystals*; O'Keefe, M., Navrotsky, A., Eds.; Academic Press: New York, 1981; Vol. 11, pp 1−30.

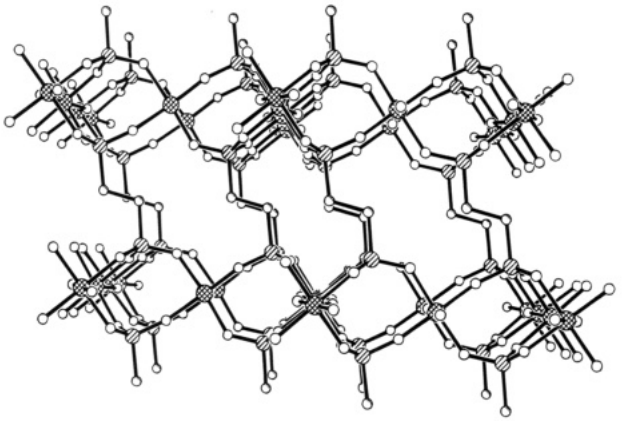

Figure 3. View of the structure of $(H_3O)_2[(VO)V_2(OH)_2(O_3PCH_2CH_2PO_3)_2]\cdot H_2O$ (**2**) down the [101] direction.

The overall structure of the anionic framework of **2** may be, likewise, characterized as inorganic V−P−O layers buttressed by the organic linkers of the diphosphonate groups, and separated by ca. 7.20 Å as shown in Figure 3. However, the details of the polyhedral connectivity within the V−P−O planes are significantly different from those described for **1**. In contrast to the structure of **1**, phase **2** contains both octahedral V(III) sites and square pyramidal V(IV) centers, illustrated in Figure 4a. This fundamental structural unit is propagated in the plane as shown in Figure 4b to give 1-dimensional chains of hydroxy-bridged V(III) octahedra linked through phosphonate tetrahedra to the square planar V(IV) sites. Thus, the V−P−O layer of **2** may be described as parallel chains of corner-sharing V(III) octahedra linked via $\{VO(O_3PR)_4\}$ groups. While linear chains of V(IV) polyhedra are observed as structural motifs in other vanadium diphosphonate phases,[30] the unit illustrated in Figure 4c is unprecedented.

The polyhedral connectivity in **2** generates cavities within the planes defined by corner-sharing of four V(III) octahedra, two V(IV) square pyramids, and six phosphonate tetrahedra. The hydronium cations occupy positions above and below these cavities and exhibit significant hydrogen-bonding interactions to the bridging −OH groups and to the vanadyl oxygens.

The coordination geometries and valence sum calculations confirm the identities of V1 and V2 as V(III) sites and V3 as a V(IV) center. The coordination geometry at the V(III) locations is defined by two bridging hydroxy groups in a trans orientation and four oxygen donors from each of four adjacent phosphonate groups. The V3 site exhibits coordination to a terminal oxo group and oxygen donors from each of four adjacent phosphonate ligands. Each $-PO_3$ terminus of the diphosphonate units serves to bridge two adjacent V(III) octahedra of a chain, utilizing the third oxygen donor to bridge to a V3 square pyramid.

While **2** represents a unique example of a V(III)/V(IV) mixed valence species for the V−O−organophosphonate system, such mixed valence species are now well-established for the corresponding $V-O-PO_4^{3-}$ system. Representative examples include $K[(V^{IV}O)V^{III}(HPO_4)_3(H_2O)_2]$,[39] $Pb_2[(V^{IV}O)V_2^{III}(PO_4)_4]$,[43] and the pyrophosphate $[(V^{IV}O)V_2^{III}(P_2O_7)_2]$.[44] However, the details of the polyhedral connectivities for these species are quite distinct from those observed for **2**.

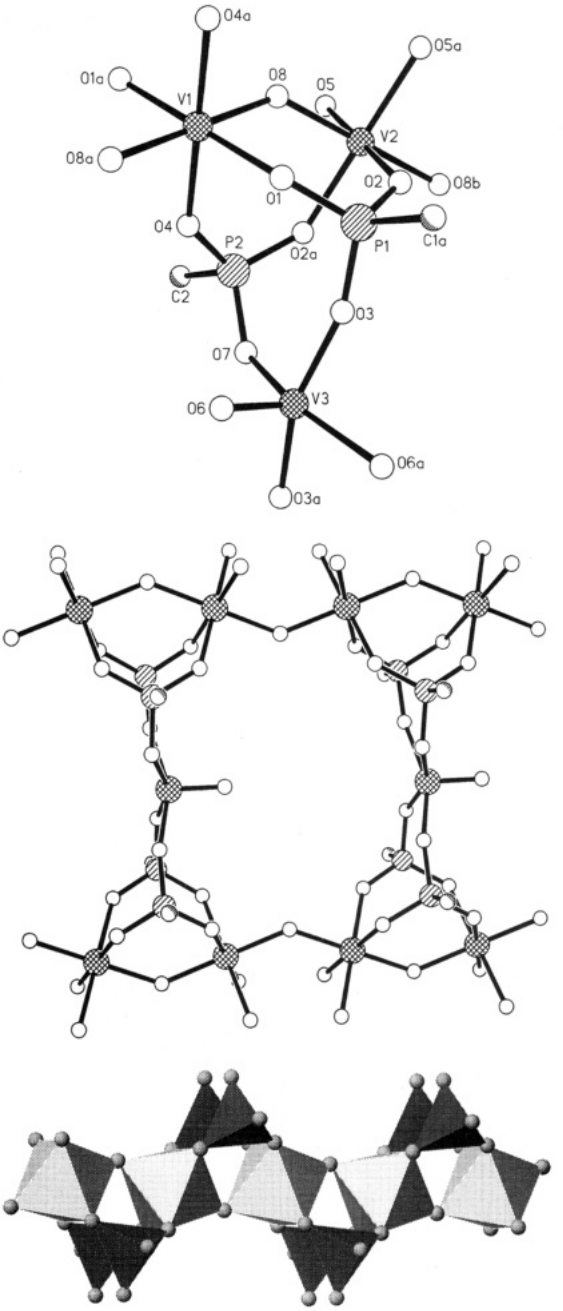

Figure 4. (a, top) Fundamental structural motif of the V−P−O layer of **2**, showing the atom-labeling scheme. (b, middle) View of the V−P−O plane of **2** which results from the propagation of the unit shown in (a). (c, bottom) Polyhedral representation of the 1-D chain of corner-sharing V(III) octahedra, symmetrically bridged by phosphorus tetrahedra, which form part of the 2-D network of **2**.

Conclusions

By exploitation of the reducing power of organoamines under hydrothermal conditions, the first two examples of phases of the $V-O-R(PO_3)_2^{4-}$ system containing V(III) centers have been isolated and structurally characterized. Oxidation states +3 through +5 have

(43) LeClaire, A.; Chardon, J.; Grandin, A.; Borel, M. M.; Raneau, B. *J. Solid State Chem.* **1994**, *108*, 291.

(44) Johnson, J. W.; Johnston, D. C.; King, H. E., Jr.; Halbert, T. R.; Brody, J. F.; Goshorn, D. P. *Inorg. Chem.* **1988**, *27*, 1646.

now been observed for this system of solid phases, and the vanadium sites adopt square-pyramidal coordination of V(IV) centers and regular or distorted octahedral geometries for V(III) or V(IV)/V(V) sites. While the solids are constructed from $\{VO_5\}$ and/or $\{VO_6\}$ polyhedra and $\{CPO_3\}$ tetrahedra through corner- and/or edge-sharing interactions, this fundamental structural motif is deceptively simple, as the details of the polyhedral connectivity allow the construction of solid lattices displaying vastly different structures. Although variations in interlayer spacing in 2-dimensional phases by exploiting the length or geometry of the organic tether are the most obvious structural modifications, the layer structure itself is dramatically variable. The inorganic V−P−O layers may contain isolated vanadium polyhedra, that is, with no V−O−V interactions, binuclear, trinuclear, and 1-dimensional chains of interacting vanadium sites. The detailed polyhedral connectivity adopted in a particular phase may produce cavities of different dimensions within the layer. Likewise, the orientations of pendant {OH} or {V=O} groups influence the relative hydrophilicity or hydrophobicity of such cavities. While the importance of cationic templates as structure directing agents is well established, a detailed understanding of template mechanism remains elusive, and the influence of a given template on product structure is generally unpredictable. As the data base of both solid phases and molecular clusters of the $V-O-RPO_3^{2-}/R'(PO_3)_2^{4-}$ systems expands, new insights into the rational synthesis of solids and supramolecular materials of this system should emerge.

Acknowledgment. This work at Syracuse University was supported by NSF Grant CHE9318824.

Supporting Information Available: Tables of atomic positional coordinates, bond lengths and angles, anisotropic temperature factors, and calculated hydrogen atom positions for **1** and **2** (11 pages); table of observed and calculated structure factors (10 pages). Ordering information is given on any correct masthead page.

CM9501067